Supporting Information

An Integrated Dual-Signal Self-Powered Flexible Sensor Based on Ferrocene-Mediated Biofuel Cell for Glucose Detection

Zheng Wang, Maruf Ahmed*, Jiayuan Zhu, Ying-zhuo Shen, Meijuan zhao, Wei Liu, Xiao-Ya Hu*, Qin Xu*

Institute of Innovation Materials and Energy, School of Chemistry and Chemical Engineering, Yangzhou University, Yangzhou 225002, China

*Corresponding authors

Tel: +86 514 87971818; Fax: +86 514 87975244

E-mail: xuqin@yzu.edu.cn

This material includes:

1. Flexibility test

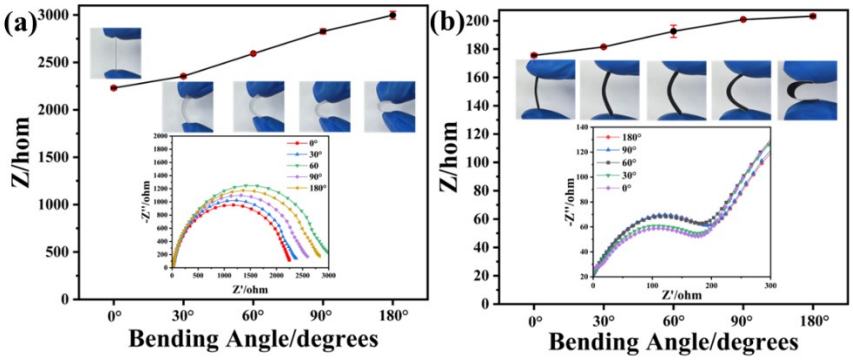

Figure S1. Resistances of (a) ITO/PET and (b) Au/CNTs-rGO film at different bending angles. Insets are the electrochemical impedance spectroscopy (EIS) and the digital photos of ITO/PET and CNTs-rGO film at different bending angles.

Electrochemical impedance spectroscopy (EIS) is used to study the resistance changes of ITO/PET and Au/CNTs-rGO film at different bending angles. **Figure S1** shows the resistances of the ITO/PET (a) and the Au/CNTs-rGO (b) at different bending angles. Notably, the nyquist impedance spectra show highly consistent shapes at different bending angles, indicating that the electrical transport processes remain stable at different bending angles. Both ITO/PET and the Au/CNTs-rGO films show small resistance changes. The results indicate that ITO/PET and the Au/CNTs-rGO films can maintain stable electrical performance after different bending angles, which can be a good candidate for flexible biosensors.

2. Optimization of sensor

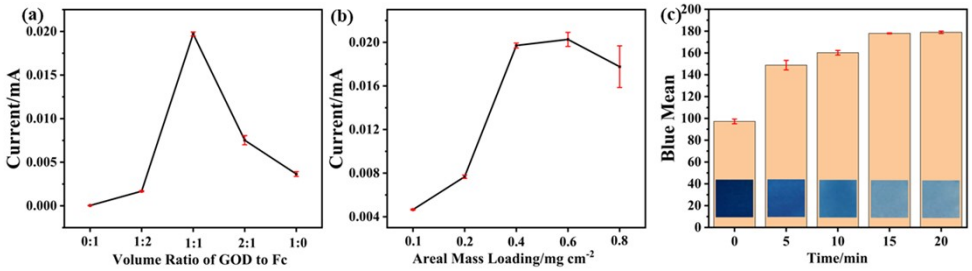

Figure S2. (a) Optimization of the volume ratio of GOD to Fc; (b) Optimization of the areal mass loading of GOD/Fc modified on the EI region; (c) Electrochromic discoloration of the EC region at different reaction times (the concentration of glucose was 80 mM).

To optimize the sensor performance, different volume ratios of GOD to Fc and loading of GOD/Fc onto the surface of EI region have been studied. **Fig S2a** shows the current exhibit a parabolic trend: it

peaks at a 1:1 ratio and declines at more extreme ratios (e.g., 1:2, 2:1, 0:1, 1:0). The observed current variation with GOD:Fc volume ratios arise from the interplay between enzymatic catalysis and electron mediation.[1] Specifically, when Fc content is low (e.g., ratios 1:2 and 0:1), the insufficient electron mediator limits electron shuttling from GOD to the electrode, reducing catalytic efficiency even with abundant GOD. Conversely, at low GOD contents (e.g., ratios 2:1 and 1:0), fewer enzymatic active sites for glucose binding and oxidation constrain the reaction, despite excess Fc. In contrast, the optimal 1:1 ratio balances GOD and Fc, enabling efficient coupling of glucose oxidation and electron transfer, thus maximizing the electrochemical current.

The loading of GOD/Fc immobilized on the surface of the EI region may affect the sensor's performance. The effects of different loading (0.1, 0.2, 0.4, 0.6, 0.8 mg cm^{-2}) on properties are shown in **Fig S2b.** At low GOD/Fc loading levels (<0.6 mg cm^{-2}), the insufficient active sites limit both glucose binding (due to sparse enzymatic active sites) and electron transfer (from scarce Fc mediators), collectively suppressing the current. Conversely, at the optimal loading levels (0.6 mg cm^{-2}), sufficient GOD/Fc loading ensures abundant active sites for glucose oxidation and ample Fc mediators for electron shuttling, synergistically facilitating efficient catalysis and electron transport to maximize the current. In contrast, high loading levels (>0.6 mg cm^{-2}) form a thick modified layer on the electrode surface, which increases electron transport resistance by elongating diffusion paths and impeding inter-molecular electron hopping among Fc species.[2] Moreover, this thick layer may physically block glucose access to GOD active sites, further attenuating the catalytic efficiency.[3]

In Fig S2c, EC region has completely faded after reaction for more than 15 min, so the accuracy and detection range of the sensor may be affected due to too long reaction time, so the optimal reaction time is 15 min. It can ensure that EC region is faded as much as possible, but it is not completely faded.

3. The real sample testing process

The feasibility of the sensor was evaluated for testing glucose in two types of real samples: serum and urine. Briefly, serum and Urine samples were diluted 10-fold by mixing 2 mL of undiluted samples with 18 mL of PBS (pH 7.4), and centrifuged at 4,000 rpm for 10 minutes to eliminate particulate matter. The standard glucose solutions with different concentrations (5 mM, 10 mM, 20 mM) were added to the real sample for recovery test which were stored at 4°C and analyzed within 2 hours to minimize analyte degradation. All samples were tested under the same conditions (37°C incubation for 15 minutes). Each sample was measured three times, and the average signal was used for calculation.

The human serum and urine experiments were approved by the Ethics Committee of Yangzhou University and were analyzed in accordance with the guidelines of the Declaration of Helsinki and all applicable ethical guidelines. All human subjects were provided with information regarding the study and gave their written informed consent prior to participation.

Table S1 Comparison of different analytical methods for glucose detection.

Electrochemical Sensor	Method	Linear Range	LOD	Reference
PCL/PPy/GO	CV[a] and DPV[b]	0.1−10 mM	18.64 μM	[4]
CNT/TTF/GDH	Amperometry	0.5–10 mM	15.26 μM	[5]
GOD-GA-Ni/Cu-MOFs-FET	Amperometry	1 μM–20 mM	0.51 μM	[6]
rGO/GOx	Amperometry	1–25 mM	0.32 mM	[7]
$FcMe_2$-LPEI/GOx	Amperometry	1–10 mM	0.48 mM	[8]
Cu-xCu_2O	DPV	0.8–10 mM	16 μM	[9]
Cu_2O	DPV	0.1–1 mM	12 μM	[10]
Nafion-GOx/GO/AZO	Potentiometry	2–10 mM	1.89 mM	[11]
cotton/ppy/Cu/Cu-Mn	DPV	50–400μM	125 μM	[12]
PQQGDH/Box	Amperometry	0.009–0.1 mM	3.2 μM	[13]
Au/PPy/PB/MWCNT/CS/GO	Amperometry	0–1 mM	12.58 μM	[14]
Pd-Cu BMA	Amperometry	1–20 mM	43.4 μM	[15]
$CuFe_2O_4$@GO	UV–vis[c]	0–1000 μM	0.79 μM	[16]
$CuFe_2O_4$@GO	visual signal	0.1–50 mM	0.04 mM	[16]

GOx@MIL-100(Fe)-B	UV–vis	5–150 μM	0.97 μM	[17]
GDH	visual signal	0–14 mM	/	[18]
GOD/Fc	Amperometry	0.1–80.0 mM	0.018 mM	**this work**
CS@PB	visual signal	0.5–80.0 M	0.36 mM	**this work**

[a] CV: cyclic voltammetry. [b] DPV: differential pulse voltammetry. [c] UV–vis: UV–vis spectrometry.

References

1. S. F. Kucukayar, S. Kaya, V. Simsek, M. O. Caglayan, Z. Ustundag and S. Sahin, *Microchemical Journal*, 2025, **208**, 112213.
2. J. Radomski, L. Vieira and V. Sieber, *Bioelectrochemistry*, 2023, **151**, 108398.
3. M. C. D. Cooray, S. Sandanayake, F. Li, S. J. Langford, A. M. Bond and J. Zhang, *Electroanalysis*, 2016, **28**, 2728-2736.
4. S. Gungordu Er, R. Bulathsinghala, S. B. Kizilates, B. Li, R. Ryan, T. A. Tabish, I. Dharmasena and M. Edirisinghe, *Advanced Science*, 2025, **12**, 2416320.
5. J. Lee, J. Ji, K. Hyun, H. Lee and Y. Kwon, *Sensors and Actuators B-Chemical*, 2022, **372**, 132647.
6. B. Wang, Y. Luo, L. Gao, B. Liu and G. Duan, *Biosensors & Bioelectronics*, 2021, **171**, 112736.
7. K. Soganci, H. Bingol and E. Zor, *Journal of Electroanalytical Chemistry*, 2021, **880**, 114801.
8. R. A. Escalona-Villalpando, A. Sandoval-Garcia, L. J. R. Espinosa, M. G. Miranda-Silva, L. G. Arriaga, S. D. Minteer and J. Ledesma-Garcia, *Journal of Power Sources*, 2021, **515**, 230631.
9. Z. Khosroshahi, F. Karimzadeh, M. Kharaziha and A. Allafchian, *Materials Science and Engineering C-Materials for Biological Applications*, 2020, **108**, 110216.
10. F. F. Franco, R. A. Hogg and L. Manjakkal, *Biosensors-Basel*, 2022, **12**, 174.
11. J.-C. Chou, S.-H. Lin, T.-Y. Lai, P.-Y. Kuo, C.-H. Lai, Y.-H. Nien and T.-Y. Su, *Sensors*, 2020, **20**, 964.
12. A. Singh, A. Sharma and S. Arya, *Journal of Analytical Science and Technology*, 2022, **13,** DOI: 10.1186/s40543-022-00320-x.
13. A. Torrinha, M. Tavares, C. Delerue-Matos and S. Morais, *Chemical Engineering Journal*, 2021, **426**, 131835.
14. G. Tian, J. Chen, D. Yang, C. Liang, Q. Zhao, Y. Liu, W. Lu and D. Qi, *Talanta*, 2025, **295**, 128428.
15. Z. Li, M. Jiang, D. Lu, Y. Wang, H. Li, W. Sun, J. Long, I. Jeerapan, J. L. Marty and Z. Zhu, *Talanta*, 2025, **287**, 127641.
16. Y. Ren, X. Zuo, Z. Liu, M. Yu, B. Zhou, Y. Xue, L. Zhu and R. Yang, *Microchemical Journal*, 2024, **206**, 111504.
17. H. Mao, H. Wang, Y. Xing, D. Wang, X. Cao, J. Yu and J. Yan, *New Journal of Chemistry*, 2025, **49**, 7237-7248.
18. N. Xiao, H. T. Li, Z. Y. Fan, F. F. Luo, D. X. Lu, W. Sun, Z. H. Li, Z. F. Wang, Y. T. Han and Z. G. Zhu, *Microchimica Acta*, 2025, **192**, 224.